Sperm induction of somatic cell-cell fusion as a novel functional test

Nicolas G. Brukman[1#], Clari Valansi[1], Benjamin Podbilewicz[1#]

[1]Department of Biology, Technion- Israel Institute of Technology, Haifa 32000, Israel

[#]Correspondence should be addressed to N.G.B. (nbrukman@gmail.com) and B.P. (podbilew@technion.ac.il).

Summary

The fusion of mammalian gametes requires the interaction between IZUMO1 on the sperm and JUNO on the oocyte. We have recently shown that ectopic expression of mouse IZUMO1 induces cell-cell fusion and that sperm can fuse to fibroblasts expressing JUNO. Here, we found that the incubation of mouse sperm with hamster fibroblasts or human epithelial cells in culture induces the fusion between these somatic cells and formation of syncytia, a pattern previously observed with some animal viruses. This sperm-induced cell-cell fusion requires a species-matching JUNO on both fusing cells, can be blocked by an antibody against IZUMO1, and does not rely on the synthesis of new proteins. The fusion is dependent on the sperm's fusogenic capacity, making this a reliable, fast and simple method for predicting sperm function during the diagnosis of male infertility.

Highlights

- Sperm induces viral-like fusion of somatic cells expressing JUNO
- We developed a new technique to determine the fertilization potential of sperm
- The test measures the capacity of sperm to induce somatic cell fusion
- The degree of somatic cell fusion correlates with the fertilizing ability of sperm

37 **Graphical abstract**

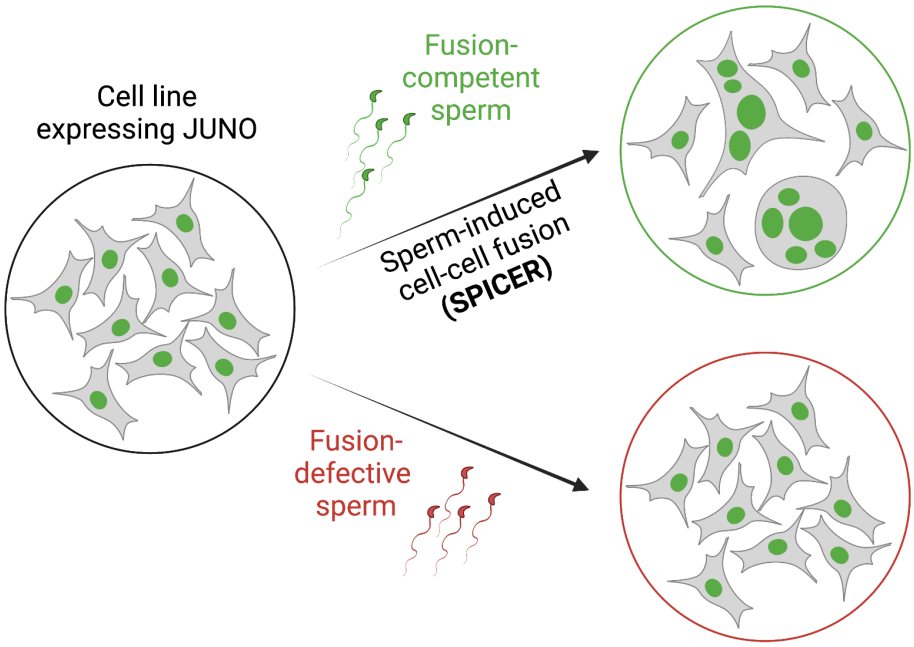

38

39 **Keywords**

40 **Male fertility test; Izumo1; Juno; in vitro fertilization (IVF); egg-sperm fusion;**
41 **assisted reproductive techniques (ART); sperm-induced cell-cell fusion**
42 **requiring JUNO (SPICER); dual split protein (DSP)**

Introduction

Infertility is estimated to affect approximately 15% of the population (World Health Organization 2023), and many couples dealing with this burden turn to assisted reproductive techniques (ARTs) as a possible solution (Steptoe and Edwards 1978; Palermo et al. 1992). During fertility evaluation of a male patient, a basic semen examination is performed, where different sperm parameters are determined: concentration, motility, morphology and vitality (World Health Organization, HRP 2021). This basic analysis can be complemented with additional tests to determine the fertilizing potential of the sperm and choose the best treatment for the couple. The hamster oocyte penetration (HOP) test has been proposed as a quantitative method for analyzing the fusogenic potential of human spermatozoa (Aitken and Elton 1986; Yanagimachi, Yanagimachi, and Rogers 1976; Zainul Rashid et al. 1998), however, it was excluded from the newest WHO laboratory manual for the examination and processing of human semen (World Health Organization, HRP 2021) for being considered obsolete. Therefore, to date there is no other standardized methodology to analyze specifically the ability of sperm to fuse to oocytes.

In mammals, the adhesion of the sperm to the oocyte plasma membranes is mediated by the species-specific interaction of two membrane proteins: IZUMO1 and JUNO (Bianchi and Wright 2015; Aydin et al. 2016; Ohto et al. 2016; Matsumura et al. 2021). The transmembrane protein IZUMO1 is expressed during spermatogenesis and localizes to the fusogenic region of the sperm head after an exocytic process named acrosome reaction (Inoue et al. 2005; Satouh et al. 2012; Inoue et al. 2015; Nishimura et al. 2016). On the other hand, the IZUMO1 receptor, JUNO, is an oocyte protein bound to the plasma membrane by a GPI lipid anchor (Bianchi et al. 2014). The subsequent fusion of the two gametes relies on the action of IZUMO1 in a unilateral manner (Brukman et al. 2023). The IZUMO1-JUNO interaction was characterized also in humans (Aydin et al. 2016; Ohto et al. 2016) and its relevance for human fertility is supported by the presence of antibodies against IZUMO1 in the sera of immuno-infertile women (Clark and Naz 2013), the mutations on JUNO in cases of fertilization failure and polyspermy (Yu et al. 2018), and the lower levels of IZUMO1 observed in sperm that failed to fertilize during *in vitro* fertilization (IVF) treatments (Enoiu et al. 2022).

Recently, we found that mouse sperm can fuse to fibroblasts ectopically expressing the sperm-receptor JUNO (Brukman et al. 2023). Here, we show that after sperm fuses with a somatic cell, this cell can fuse with additional cells inducing syncytia formation - a single cell with several nuclei (multinucleated cell). This is likely mediated by the transfer of the fusion machinery from the sperm to the target somatic cell. We call this process “SPerm-Induced CEll-cell fusion Requiring JUNO” (SPICER). We found that sperm with higher fertilizing ability can induce the fusion of somatic cells more efficiently, judged by the increased levels of multinucleation. Therefore, the number and size of these syncytia can indicate the fertilizing potential of the sperm

and can help embryologists to better predict the success of the different ARTs for each individual. Based on this, we propose a new method for diagnosis of male fertility based on the ability of sperm to induce cell-cell fusion *in vitro*.

Results

Sperm fusion to fibroblasts promotes syncytia formation

There are reports showing that mammalian sperm can fuse to somatic cells (Rival et al. 2019; Mattioli et al. 2009; Bendich, Borenfreund, and Sternberg 1974). In our experimental conditions, mouse sperm cells only fuse to Baby Hamster Kidney (BHK) cells if they are induced to express the sperm-receptor, JUNO (Brukman et al. 2023). This fusion was demonstrated by detecting the transfer of the DNA binding GFP (GFP-MBD) from the BHK cells to the sperm heads (Brukman et al. 2023). To further study the mechanisms of mammalian sperm-oocyte fusion, we incubated mouse sperm with BHK cells expressing JUNO (functioning as pseudo-oocytes) and determined the efficiency of the sperm-BHK cell interactions. Surprisingly, we found that sperm induces the formation of multinucleated BHK cells (syncytia; Fig. 1A-C). The induction of multinucleation was dependent on the presence of JUNO (Fig. 1B-C), however, JUNO expression alone is not sufficient to induce this process. Only cells with sperm fused to them form syncytia (Fig. 1C). Thus, the fusion of sperm with JUNO-expressing BHK cells is required for inducing subsequent multinucleation of these somatic cells. This phenomenon was unexpected, leading us to further study the mechanisms of this process.

Sperm induce syncytia formation using a viral-like mechanism

To our knowledge, sperm-induced cell-cell fusion has not been described in any species. However, decades ago, it was first described that some somatic cells can fuse following viral infection (Okada 1962; Kohn 1965) and later confirmed for diverse viruses, including SARS-CoV2 (Buchrieser et al. 2020). This process may require the synthesis of new viral proteins and therefore induces Fusion From Within (FFWI) while other viruses induce fusion independently of protein synthesis in a process called Fusion From Without (FFWO) (Bratt and Gallaher 1969; Duelli and Lazebnik 2007). For instance, orthoreoviruses induce the expression of fusion-associated small transmembrane (FAST) proteins upon infection, promoting FFWI (Ciechonska, Key, and Duncan 2014; Theuerkauf et al. 2021). We hypothesized that in a way reminiscent of viral induced cell-cell fusion, sperm could induce syncytia formation following its merger via FFWI or FFWO. To distinguish between these alternative mechanisms, we performed the experiment in the presence of cycloheximide to inhibit protein synthesis. We found no differences in the levels of multinucleation between control and cycloheximide treatments (Fig 1B and D). This shows that *de novo* protein synthesis is not required for the induction of multinucleation by sperm and suggests a mechanism of FFWO. Additionally, live imaging of the process showed that fusion between cells occurs efficiently within 10-15 minutes after the addition of the sperm

124 (Fig. 1E, Movie S1), suggesting that protein synthesis is not involved. We have
125 previously shown that IZUMO1 fades from the sperm after fusion to the fibroblast
126 (Brukman et al. 2023) indicating that this transmembrane protein is transferred to the
127 target cell plasma membrane. Consistent with these findings, IZUMO1 was observed
128 diffusing to the oocyte plasma membrane during in vitro fertilization assays (Satouh et
129 al. 2012). Here we detected IZUMO1 by immunostaining and by a fluorescent reporter
130 and confirmed that it diffuses from the sperm head after its fusion with the BHK cell
131 (Fig. S1A-B), suggesting a critical function for the fusogenic machinery carried by the
132 sperm during the FFWO process. Thus, sperm-BHK fusion appears to trigger BHK-
133 BHK cell fusion, observed as multinucleation, without the requirement of *de novo*
134 synthesis of proteins, likely by passing the sperm's fusogenic machinery onto the BHK
135 cells. In this sense, two models may explain FFWO induced by sperm (Fig. S1C),
136 similarly to what was reported for viruses (Tang et al. 2021). The first model involves
137 an initial fusion of the sperm to a BHK cell expressing JUNO, the transfer of IZUMO1
138 to the target cell (forming a pseudo-sperm from a pseudo-oocyte) and a subsequent
139 fusion to a new JUNO-expressing BHK (Fig. S1Ci). On the other hand, the second
140 model suggests the fusion of one sperm cell with two JUNO-positive BHK cells,
141 bridging both and forming a continuous syncytium (Fig. S1Cii). At the moment, we
142 cannot exclude either model, or their coexistence. Even though it is not known whether
143 sperm can induce fusion of somatic cells *in vivo*, we show that sperm use a viral-like
144 mechanism of FFWO when the fibroblasts express the oocyte JUNO *in vitro*.

145 **Syncytia formation results from the fusion of cells expressing JUNO**

146 Then we asked whether the sperm-induced multinucleation was a consequence
147 of BHK-BHK fusion and if so, whether it requires JUNO to be present on both fusing
148 cells. For that, we employed a content mixing experiment where two populations of
149 cells expressing different fluorescent markers were mixed and then exposed to sperm
150 (Fig. 2A). We observed the formation of multinucleated hybrid cells containing both
151 fluorescent markers, confirming the fusion of BHK cells expressing JUNO (Fig. 2B).
152 This BHK-BHK fusion was not observed when only one or neither of the cell
153 populations expressed JUNO (Fig. 2B-C), indicating that sperm-induced
154 multinucleation is indeed BHK-BHK fusion which relies on bilateral expression of
155 JUNO. An alternative explanation for sperm-induced multinucleation is a failure in
156 cytokinesis. However, the presence of an inhibitor of the cell cycle (FdUdr, 5-fluoro-2′-
157 deoxyuridine, (Valansi et al. 2017)) does not inhibit multinucleation (Fig. 3A-B), ruling
158 out that syncytia formation is as a consequence of failure in the division of the BHKs
159 and confirming the occurrence of fusion between them. Following these findings, we
160 named this process SPICER that stands for "SPerm-Induced CEll-cell fusion Requiring
161 JUNO".

162 **Sperm-induced multinucleation as a readout of sperm fertilizing ability**

163 Following the discovery of the ability of sperm to induce cell-cell fusion, we decided
164 to evaluate whether BHK multinucleation could be used as a readout of sperm

fusogenic potential. For this purpose, we incubated the sperm in media lacking BSA or Ca^{2+} that do not support capacitation (i.e. a process by which sperm acquires its fusogenic activity) (Visconti et al. 1995; Yanagimachi 1988). We found that sperm cells incubated under these conditions failed to fuse to BHK cells, as well as to induce syncytia formation (Fig 3A-B). Thus, BHK-BHK cell fusion requires fully capacitated sperm. A sperm which is unable to fuse with BHK cells, will not induce subsequent multinucleation.

SPICER depends on the activity of IZUMO1

The sperm IZUMO1 protein is essential for sperm-egg interactions via binding to JUNO (Bianchi et al. 2014). More recently, IZUMO1 was shown to induce fusion of cells in a JUNO-independent way using a different domain that is not required for binding to the egg receptor (Brukman et al. 2023). To study whether IZUMO1 is required for the fusion of sperm to BHK cells and for the induction of multinucleation of the fibroblasts, we decided to inhibit IZUMO1 activity using a blocking antibody. For this purpose, we used a monoclonal antibody against IZUMO1 which has been shown to inhibit sperm-egg fusion (Inoue et al. 2013) in our sperm-induced multinucleation assay. We found that the anti-IZUMO1 antibody had the ability to block both sperm-BHK and sperm-induced BHK-BHK fusions even when sperm cells were fully capacitated (Fig 3A-B). Altogether, our results show that the SPICER assay is able to determine sperm fertilization potential that depends on the IZUMO-JUNO interactions.

Cell-cell fusion requires species-specific JUNO

Elegant work on IZUMO1-JUNO interactions among different mammalian species has shown species-specific selectivity between these crucial interactions (Bianchi and Wright 2015). To evaluate the effect of species-specificity of the SPICER assay, we incubated the mouse sperm with BHK cells expressing human JUNO. Under these conditions, we observed lower levels of sperm-BHK fusion and a reduction in BHK multinucleation compared to cells expressing mouse JUNO (Fig 4A-C). Interestingly, the low activity mediated by human JUNO was still significant compared to the control without JUNO. This confirms the requirement of a species-matching JUNO for the assay; however, it puts in evidence a residual cross-interaction between mouse sperm and human JUNO.

Sperm induce the fusion of human epithelial cells

To exclude any BHK cell-specific requirement for SPICER, we tested the epithelial human embryonic kidney 293T (HEK) cells. Due to the smaller size and more rounded shape of these cells that hinder the quantification of multinucleation, we opted to analyze fusion by content mixing. For this, we utilized the Dual Split Protein system (Wang et al. 2014; Ishikawa et al. 2012) which employs two GFP halves expressed in different populations of cells. Upon fusion of these two populations, the reporter self-assembles and the cells become fluorescent (Nakane and Matsuda 2015). The

204 number of green fluorescent cells relative to the number of transfected cells was
205 determined as an indication of fusion levels (Fig. 5A). As observed for the BHK cells,
206 HEK cells bearing JUNO fused between them when they were co-incubated with
207 sperm (Fig. 5B-C). On the contrary, neither HEK cells without JUNO nor HEK
208 expressing JUNO but without sperm showed content mixing (Fig. 5B-C). These results
209 show that SPICER is not restricted to BHK cells or fibroblasts and opens the possibility
210 for adapting this assay to different cell lines and approaches to evaluate cell-cell
211 fusion.

212 **Discussion**

213 **SPICER as a diagnostic tool**

214 Determining sperm's fusogenic potential is of great interest for infertility diagnosis
215 of both human and stud animals. Considering that the hamster oocyte penetration
216 (HOP) assay became obsolete, an assay that evaluates the fusion of somatic cells
217 with ectopic expression of JUNO induced by competent sperm (SPICER, Fig. 6)
218 represents a powerful diagnostic tool. SPICER could predict the success chances of
219 ARTs like intrauterine insemination (IUI) or conventional IVF, which require a fusion-
220 competent sperm and if it is necessary to proceed with a more complex technique
221 such as intracytoplasmic sperm injection (ICSI). This is particularly important
222 considering the routine use of the ICSI is under debate as it is associated with a slightly
223 higher risk of adverse outcomes in the progeny (Practice Committees of the American
224 Society for Reproductive Medicine and the Society for Assisted Reproductive
225 Technology 2020).

226 Considering our previous work showing that IZUMO1 can mediate cell-cell fusion
227 (Brukman et al. 2023) and that significantly lower levels of this protein were detected
228 in the sperm cells from patients with total fertilization failure (Enoiu et al. 2022), we
229 expect that the SPICER assay will be able to resolve some unexplained cases of male
230 infertility that result from loss of function of components of the fusion machinery. In this
231 context, other proteins that are essential for gamete fusion, such as SPACA6,
232 TMEM95, FIMP, SOF1 and DCST1/2 (Barbaux et al. 2020; Noda et al. 2020;
233 Lorenzetti et al. 2014; Lamas-Toranzo et al. 2020; Fujihara et al. 2020; Inoue,
234 Hagihara, and Wada 2021; Noda et al. 2022), might be transferred to the somatic cells
235 together with IZUMO1 during sperm-induced cell-cell fusion. Finally, considering that
236 antibodies against IZUMO1 were detected on the sera of infertile women (Clark and
237 Naz 2013) and here we observed that a monoclonal antibody against this protein was
238 able to block sperm-induced syncytia, SPICER could serve as tool to readily analyze
239 cases of immuno-infertility.

240 **SPICER occurrence *in vivo***

241 Apart from being expressed in oocytes, JUNO has been described in lymphoid
242 tissues (Spiegelstein, Eudy, and Finnell 2000), more specifically in regulatory T cells

(Yamaguchi et al. 2007). Therefore, we cannot exclude that sperm could bind and fuse to other cell types *in vivo*, and whether it has any physiological or pathological relevance. This fusion cannot occur before acrosomal exocytosis, when IZUMO1 is enclosed into the acrosome (Inoue et al. 2005; Satouh et al. 2012), and therefore, it will be relevant to study sperm fusion to somatic cells within the oviduct of the female, close to the fertilization site (Muro et al. 2016; Hino et al. 2016; La Spina et al. 2016). Furthermore, JUNO was detected in the first polar body (Suzuki et al. 2017) and whether sperm can fuse to it or if sperm fusion to the oocyte can induce the polar body-egg fusion remains unknown.

Expanding SPICER across species

The assay that we described here can be a potent tool to study cross-fertilization between different species and mechanisms of speciation and evolution, presenting a step beyond biochemical approaches to study IZUMO1-JUNO interactions (Bianchi and Wright 2015; Nakajima et al. 2022). On the other hand, by simply exchanging the JUNO sequence used, this assay could be easily adapted to allow the analysis of the sperm fertilizing ability in different mammalian species, such as humans or cattle, having implications not only for reproductive health but also for biotechnological and agricultural uses. Furthermore, even though IZUMO-JUNO interaction is a specific requirement during sperm-egg fusion of mammals (Grayson 2015), we cannot exclude that alternative configurations, using the right egg receptors (Lu and Ikawa 2022), will be possible in the future to induce somatic cell-cell fusion by sperm of other sexually reproducing organisms. In species where *Izumo1* and *Juno* genes are absent, such as plants and protists, the gamete fusion is promoted by the fusogen HAPLESS 2/GENERATIVE CELL-SPECIFIC 1 (HAP2/GCS1) (Brukman, Li, and Podbilewicz 2022). In other organisms like zebrafish or nematodes, IZUMO1 orthologs were described (Binner et al. 2021; Nishimura et al. 2015; Takayama et al. 2021) but, since JUNO is present only in mammals (Vance and Lee 2020; Grayson 2015), it is unclear whether male gametes in other species interact with different receptors on the female gamete. Therefore, it can be speculated, for instance, that the expression of a species-specific Bouncer will be required to activate the fusion of fish sperm (Gert et al. 2023; Herberg et al. 2018) or *Chlamydomonas* FUS1 to mediate the fusion of the algae minus gamete (Pinello, Liu, and Snell 2021; Ferris, Woessner, and Goodenough 1996).

Further applications for SPICER

In addition to the potential uses of SPICER for diagnosis of infertility, this assay could be used to evaluate potential sperm donors and animal studs. Moreover, our SPICER tool has the potential to aid screening for compounds that enhance fertilization (new fertility treatments) or that block gamete interactions (Stepanenko et al. 2022), or to easily determine the effect of genetic variations of JUNO (Allingham and Floriano 2021; Takaiso et al. 2016). SPICER could also facilitate studies aimed at resolving standing enigmas of sperm-egg fusion (Deneke and Pauli 2021;

284 Yanagimachi 2022). This includes the role of IZUMO1 and other potential fusogens as
285 well as additional cellular pathways that are known to influence fusion in different
286 systems, including the action of the cytoskeleton and molecular motors (Shilagardi et
287 al. 2013; Yang et al. 2017; Zhang et al. 2017), specific lipids (e.g. phosphatidylserine)
288 (Rival et al. 2019; van den Eijnde et al. 2001; Verma et al. 2018; Abay et al. 2017),
289 calcium signaling (Tsuchiya et al. 2018; Earles et al. 2001), phosphorylation cascades
290 (Eigler et al. 2021) and more (Brukman et al. 2019). Finally, whether other cell types
291 rather than sperm, such as muscle cells or osteoclasts, can induce syncytia formation
292 after ectopic fusion remains an open question, with important biological implications.

293 **Limitations of the study**

294 The main caveat of our assay is that it cannot discriminate between defects in
295 sperm docking or gamete fusion, as a poor performance in SPICER could be explained
296 by the altered interaction of IZUMO1 and JUNO or by a reduced capacity of IZUMO1
297 (and IZUMO1 partners in the sperm) to induce membrane merger. Moreover,
298 simultaneous measurements of the levels of spontaneous acrosome reaction will be
299 needed to exclude a faulty capacitation. Alternatively, capacitation could be further
300 stimulated pharmacologically using a Ca^{2+} ionophore (Tateno et al. 2013). In this
301 context, further analysis may be required to refine the characterization of defective
302 sperm. Lastly, the exact pathway for the FFWO mediated by the sperm will be a
303 subject of future investigations.

304 **MATERIALS AND METHODS**
305
306 **KEY RESOURCES TABLE**
307

REAGENT or RESOURCE	SOURCE	IDENTIFIER
Antibodies		
Anti-IZUMO1 Mab120 monoclonal antibody	Merck Millipore	Cat# MABT1357
Anti-goat IgG secondary antibody, Alexa Fluor 647	Thermo Fisher Scientific	Cat# A-21247, RRID: AB_141778
Bacterial and virus strains		
DH5α competent cells	Thermo Fisher Scientific	Cat# 18265017
Chemicals, peptides, and recombinant proteins		
jetPRIME® transfection reagent	Polyplus Transfection	Cat# 101000046

FdUdr, 5-Fluoro-2'-deoxyuridine	Sigma	Cat# F0503, CAS: 50-91-9
BSA, bovine serum albumin	Sigma	Cat# A7906, CAS: 9048-46-8
Hyaluronidase	Sigma	Cat# H3506, CAS: 37326-33-3
Cycloheximide	Sigma	Cat# C7698, CAS: 66-81-9
Puromycin Dihydrochloride	GoldBio	Cat# P-600-100, CAS: 58-58-2
Poly-L-lysine hydrobromide	Sigma	Cat# P2636, CAS: 25988-63-0
Experimental models: Cell lines		
BHK-21, clone 13	ATCC	Cat# CCL-10, RRID: CVCL_1915
HEK293T	ATCC	Cat# CRL-3216, RRID:CVCL_0063
HEK293T-DSP1-7	This paper	N/A
HEK293T-DSP8-11	This paper	N/A
Experimental models: Organisms/strains		
B6D2.C57BL/6-Tg(Zp3-EGFP/Cd9)1Osb mouse line	(Satouh et al. 2012)	N/A
FVB/129sv/CF1	This paper	N/A
Oligonucleotides		
IZUMO1-mCherry F (Genotyping): CCTTCCTGCGGCTTGTTCTCT	(Satouh et al. 2012)	N/A

IZUMO1-mCherry R (Genotyping): ATCAAGGTCTCAGAACTGTTCTC CCAAACC	(Satouh et al. 2012)	N/A
NheI Human Juno (Cloning into pCI::H2B-RFP): TTATCGCTAGCATGGCATGCTGGTGGCC GCTC	This paper	N/A
EcoRV Human Juno R (Cloning into pCI::H2B-RFP): CCAGGATATCTCAGGAAAGGAACGGCAG GAAC	This paper	N/A
Recombinant DNA		
pCI::H2B-RFP	(Williams et al. 2018)	Addgene #92398
pCI::GFPnes	(Moi et al. 2022)	N/A
pCI::mJUNO::H2B-RFP	(Brukman et al. 2023)	N/A
pCI::mJUNO::GFPnes	(Brukman et al. 2023)	N/A
pcDNA3.1-EGFP-MBD-nls	(Yamagata et al. 2005)	N/A
pCMV6-humanJUNO	(Wood and Wright 2019)	N/A
pCI::humanJUNO::H2B-RFP	This paper	N/A
pIRESpuro3-DSP1–7	(Wang et al. 2014)	N/A
pIRESpuro3-DSP8-11	(Wang et al. 2014)	N/A
Software and algorithms		
GraphPad Prism 9	GraphPad Prism	RRID:SCR_002798
FIJI (ImageJ 1.53c)	Image J	RRID:SCR_002285
Photoshop CS6	Adobe	RRID:SCR_014199
Illustrator CS6	Adobe	RRID:SCR_010279
ZEN microscopy software 7.0.4.0	ZEISS	RRID:SCR_013672

MetaMorph image analysis software 7.8.1.0	Molecular Devices	RRID:SCR_002368
Biorender	Biorender	RRID:SCR_018361

RESOURCE AVAILABILITY

Lead contact

Further information and requests for resources and reagents should be directed to and will be fulfilled by the lead contact, Benjamin Podbilewicz (podbilew@technion.ac.il).

Materials availability

Plasmids or cell lines generated in this study are available upon request. Signing a materials transfer agreement (MTA) may be required.

Data and code availability

Any additional information required to reanalyze the data reported in this paper is available from the lead contact upon request.

EXPERIMENTAL MODEL AND SUBJECT DETAILS

Animals

All animal studies were approved by the Committee on the Ethics of Animal Experiments of the Technion - Israel Institute of Technology. In this study, we used wild-type male mice from a FVB/129sv/CF1 mixed background and B6D2-Tg(Izumo1-mCherry) mouse line (Satouh et al. 2012). Animals were bred and housed in the Technion animal facility under specific pathogen–free conditions with *ad libitum* access to food and water. The primers used for genotyping Izumo1-mCherry are outlined in the Key Resources Table. In all cases, male mice between 3 and 6 months old were used for the experiments.

Cell lines and DNA transfection

BHK cells (Cat# CCL-10; ATCC, RRID: CVCL_1915) and HEK293T cells (Cat# CRL-3216; ATCC, RRID: CVCL_0063) were grown and maintained in DMEM containing 10% FBS. Cells were cultured at 37°C in 5% CO_2. Plasmids were transfected into cells using 2 µl jetPRIME (PolyPlus-transfection) per µg of DNA in 100 µl of reaction buffer for every ml of medium. HEK293T cells stable lines for Dual Split Proteins (DSP) 1-7 and 8-11 were prepared by transfecting pIRESpuro3-DSP1–7 and pIRESpuro3-DSP8-11 respectively and selecting with 2 µg/ml of puromycin for 10–13 days as previously described (Wang et al. 2014).

METHOD DETAILS

342 **Sperm collection and capacitation**

343 Sperm were recovered by incising the cauda epididymis, obtained from adult male
344 mice, in 300 µl of mHTF medium (Kito et al. 2004) supplemented with 4 mg/ml of BSA.
345 The sperm were diluted in fresh medium to a concentration of 5 × 10^6 cells/ml and
346 incubated for 90 min at 37°C and 5% CO_2 to induce capacitation.

347 **Sperm-to-BHK fusion and multinucleation**

348 BHK cells were grown on 24-well glass bottom tissue-culture plates. 24 h after
349 plating, cells were transfected with 0.25 µg pcDNA3.1-EGFP-MBD-nls plasmids and
350 0.5 µg of either pCI::H2B-RFP or pCI::JUNO::H2B-RFP. 24 h after transfection, 2 ×
351 10^6 capacitated wild-type sperm cells in mHTF were added to each well and co-
352 incubated with the BHK cells for 4 h at 37°C and 5% CO_2. After one wash with PBS,
353 the cells were fixed with 4% PFA in PBS and stained with 1 µg/ml DAPI. Micrographs
354 were obtained using wide-field illumination using an ELYRA system S.1 microscope
355 (Plan-Apochromat 20× NA 0.8; Zeiss). Multinucleation percentage was determined as
356 the ratio between the number of nuclei in multinucleated cells (NuM) and the total
357 number of nuclei in fluorescent cells (NuF), as follows: % of multinucleation =
358 (NuM/NuF) × 100. 500 nuclei (NuF) were counted in each independent repetition
359 (experimental point). In some cases, the number of sperm fused was determined by
360 evaluating the transfer of EGFP-MBD-nls signal from the BHK cell to the sperm nuclei
361 (number of fused sperm/500 BHK cells). In some experiments, sperm cells obtained
362 from transgenic mice expressing IZUMO1-mCherry were employed to analyze
363 IZUMO1 localization.

364 **Content mixing assay using different colors**

365 BHK cells at 70% confluence in 35-mm plates were transfected with 1 µg
366 pCI::H2B-RFP, pCI::GFPnes, pCI::JUNO::H2B-RFP or pCI::JUNO::GFPnes. 4 h after
367 transfection, the cells were washed four times with DMEM with 10% serum, four times
368 with PBS, and detached using Trypsin (Biological Industries). The cells were collected,
369 resuspended in DMEM with 10% serum, and counted. Equal amount of H2B-RFP and
370 GFPnes cells (1.25 × 10^5 each) were mixed and seeded on glass-bottom plates (12-
371 well black, glass-bottom #1.5H; Cellvis) and incubated at 37°C and 5% CO_2. 18 h after
372 mixing, 4 × 10^6 capacitated wild-type sperm cells in mHTF were added to the BHK
373 cells and co-incubated for 4 h after which they were washed with PBS, fixed with 4%
374 PFA in PBS and stained with 1 µg/ml DAPI. Micrographs were obtained using wide-
375 field illumination using an ELYRA system S.1 microscope (Plan-Apochromat 20× NA
376 0.8; Zeiss). The percentage of mixing was defined as the ratio between the nuclei in
377 mixed cells (NuM) and the total number of nuclei in mixed cells and fluorescent cells
378 in contact that did not fuse (NuC), as follows: % of mixing = (NuM/[NuM + NuC]) × 100.
379 1,000 nuclei (NuM + NuC) were counted in each independent repetition (experimental
380 point).

381 **Content mixing assay using the Dual Split Protein**

382 Equal amount of HEK293T cells stably expressing DSP1-7 or DSP8-11 were
383 mixed (1.25 × 10^5 each) and seeded on glass-bottom plates (12-well black, glass-
384 bottom #1.5H; Cellvis) pre-treated with 20 µg/ml of Poly-L-lysine. 24 h later, the cells
385 were transfected with 1 µg pCI::H2B-RFP or pCI::JUNO::H2B-RFP. 18 h after
386 transfection, 4 × 10^6 capacitated wild-type sperm cells in mHTF were added to the
387 HEK293T cells and co-incubated for 4 h after which they were washed with PBS, fixed
388 with 4% PFA in PBS and stained with 1 µg/ml DAPI. Micrographs were obtained as
389 above, using wide-field illumination using an ELYRA system S.1 microscope (Plan-
390 Apochromat 20× NA 0.8; Zeiss). The number of GFP positive cells per 1,000 nuclei
391 was determined. Between 1,000 to 2,000 red nuclei were counted in each independent
392 repetition (experimental point).

393 **Inhibition of sperm-induced cell-cell fusion**

394 Different conditions were tested to evaluate their effect on sperm-induced cell-cell
395 fusion. Non-capacitated sperm were incubated in medium mHTF lacking Ca^{2+} or BSA
396 for 90 min at 37°C and 5% CO_2. In other cases, capacitated sperm were mixed before
397 their addition to the BHK cells with 1 µg/µl of anti-IZUMO1 antibody (Inoue et al. 2013),
398 20 µM of the cell cycle inhibitor FdUdr (Valansi et al. 2017) or 200 µg/ml of the inhibitor
399 of protein synthesis cycloheximide (Wengler 1975).

400 **Time-lapse Imaging of sperm induced cell-cell fusion**

401 BHK cells were grown on 35 mm glass bottom tissue-culture plates (Greiner Bio-
402 one) and, 24 h after plating, cells were transfected with 1.5 µg pCI::JUNO::GFPnes. 24
403 h after transfection, time-lapse images of the cells were imaged before and after
404 adding 5 × 10^6 capacitated wild-type sperm cells in mHTF. Images of the cells were
405 acquired every 3 min for 1 h to record cell-to-cell fusion, using a spinning disc confocal
406 microscope (CSU-X; Yokogawa Electric Corporation) with an Eclipse Ti inverted
407 microscope and a Plan-Apochromat ×20 (NA, 0.75; Nikon) objective. Images were
408 obtained using an iXon3 EMCCD camera (ANDOR) through MetaMorph (Molecular
409 Devices, version 7.8.1.0). Images in differential interference contrast and green
410 channels were recorded.

411 **Immunofluorescence**

412 The localization of IZUMO1 was determined by immunostaining. Briefly, after
413 fixation cell were permeabilized with 0.1% Triton X-100 in PBS and incubated with
414 anti-IZUMO1, clone Mab120 (1:500, Cat# MABT1357; Merck Millipore) followed by the
415 secondary antibody Alexa Fluor 647 goat anti-rat (1:500, Cat# A-21247; Thermo
416 Fisher Scientific, RRID: AB_141778). Later, the nuclei were stained with 1 µg/ml DAPI
417 and micrographs were obtained using wide-field illumination using an ELYRA system
418 S.1 microscope (Plan-Apochromat 20× NA 0.8; Zeiss) with an EMCCD iXon camera

(Andor) through ZEN microscopy software 7.0.4.0 (RRID: SCR_013672; Zeiss).

QUANTIFICATION AND STATISTICAL ANALYSIS

Statistics and data analysis

Results are shown as means ± SEM. For each experiment, at least three independent biological repetitions were performed. The significance of differences between the averages were analyzed using one-way ANOVA as described in the legends (GraphPad Prism 9, RRID: SCR_002798). Figures were prepared with Photoshop CS6 (Adobe, RRID: SCR_014199), Illustrator CS6 (Adobe, RRID: SCR_010279), BioRender.com (RRID: SCR_018361), and FIJI (ImageJ 1.53c, RRID: SCR_002285).

Acknowledgements

We thank Gavin Wright (University of York, York, UK) for the pCMV6-hJuno plasmid, Kazuo Yamagata (Kindai University, Higashiosaka City, Osaka, Japan) for the EGFP-MBD-NLS plasmid, Masahito Ikawa (Osaka University, Osaka, Japan) for the IZUMO1-mCherry transgenic mouse line, and Zene Matsuda (University of Tokyo, Japan) for the DSP plasmids. Finally, we thank Dan Cassel (Technion- Israel Institute of Technology), Leonid Chernomordik (NICHD/DIR, NIH, US) and the members of Podbilewicz Lab for critically reading the manuscript.

This project has received funding from the Israel Science Foundation (257/17, 2462/18, 2327/19, and 178/20 to B. Podbilewicz) and the European Union's Horizon 2020 research and innovation program under the Marie Skłodowska-Curie Actions (844807 to N.G. Brukman).

Author contributions

B.P. conceived the study. N.G.B. and C.V. designed and conducted experiments, and processed and analyzed the data supervised by B.P.; N.G.B. wrote the initial draft of the manuscript. All authors participated in discussions of results and manuscript editing.

Declaration of interests

N.G.B., C.V. and B.P. are inventors on a patent application filed by the Technion- Israel Institute of Technology, based on this work.

450 **Figures**

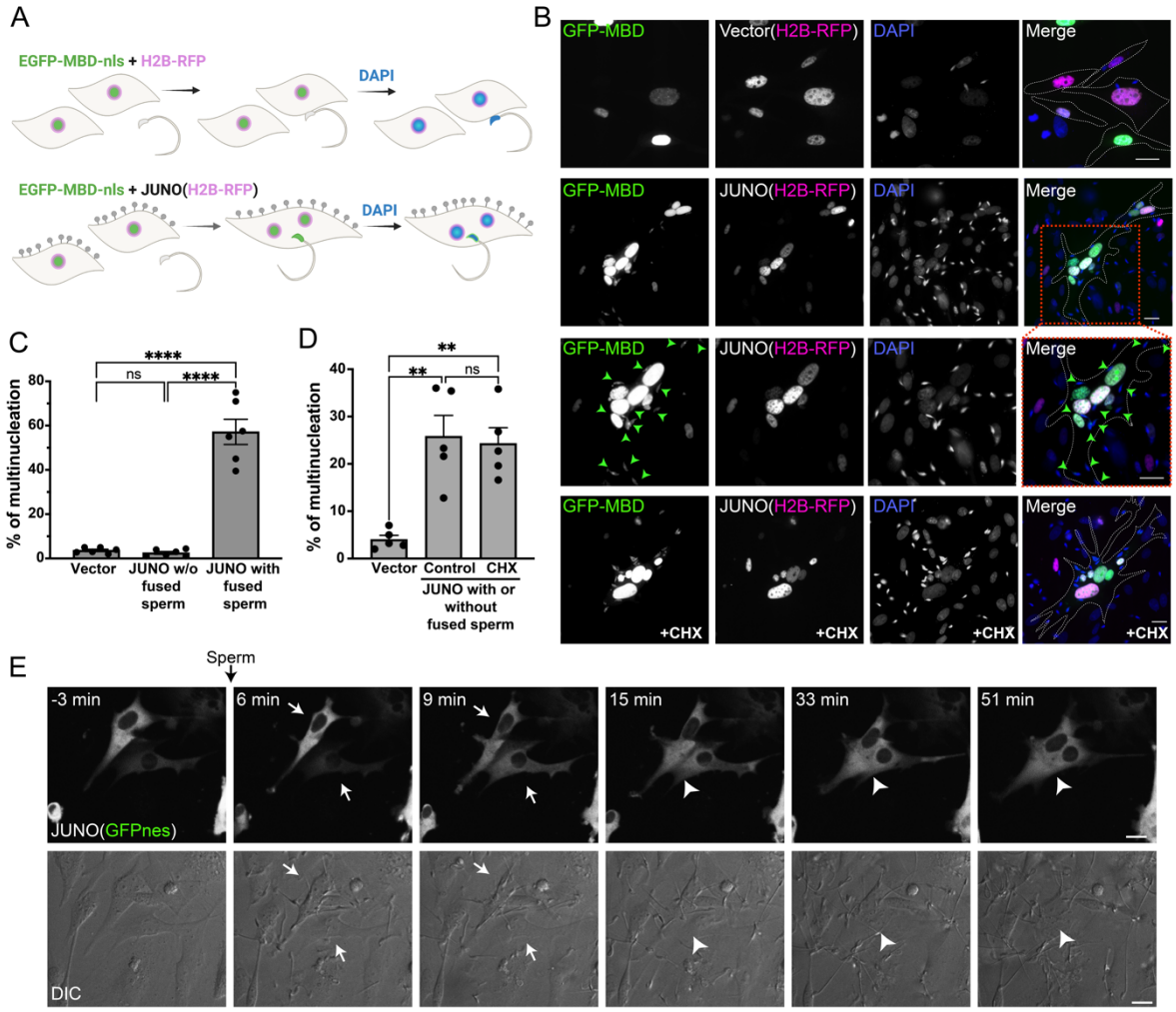

451

452 <u>Figure 1: Sperm induce syncytia formation of fibroblasts</u>

453 **(A)** Scheme of experimental design: Baby Hamster Kidney (BHK) cells were
454 transfected with either pCI::H2B-RFP or pCI::JUNO::H2B-RFP vectors and
455 pcDNA3.1-EGFP-MBD-nls. Mouse sperm were obtained from the epididymis of adult
456 mice and capacitated in HTF capacitating medium. Sperm cells were co-incubated
457 with the BHK cells for 4 h and then the cells were fixed and stained with DAPI to detect
458 the DNA. Grey lollipops represent JUNO molecules **(B)** Representative images
459 showing H2B-RFP (magenta), GFP-MBD (green), DAPI (blue) channels and the
460 merge. Dotted lines contour relevant cells. Green arrowheads point to fused sperm
461 (GFP positive). The presence of 200 µg/ml of cycloheximide is indicated (CHX). Scale
462 bars, 20 µm. **(C)** The percentage of multinucleation was defined as the ratio between
463 the nuclei in multinucleated cells (NuM) and the total number of nuclei in fluorescent
464 cells (NuF), as follows: % of multinucleation = (NuM/NuF) × 100. We show individual
465 data and means ± SEM of six independent experiments. The number of nuclei counted
466 per experiment and per treatment was 500. For JUNO transfected cells,
467 multinucleation was counted separately for cells with and without sperm fused to them.

468 Comparisons were made with one-way ANOVA followed by Tukey's test. ns = non-
469 significant, ****P < 0.0001. **(D)** In another set of experiments JUNO-transfected cells
470 were treated with 200 µg/ml CXH to inhibit *de novo* synthesis of proteins. We show
471 individual data and means ± SEM of five independent experiments. ns = non-
472 significant, **P < 0.01. **(E)** Time-lapse images from a movie showing sperm-induced
473 cell-cell fusion. BHK cells were transfected with the pCI::JUNO::GFPnes plasmid and
474 sperm were added at time=0 min. Arrows and arrowheads indicate contacting and
475 fused cells, respectively. The green channel (GFPnes) and the DIC images are shown
476 (see also Movie S1). Scale bars, 20 µm.

477

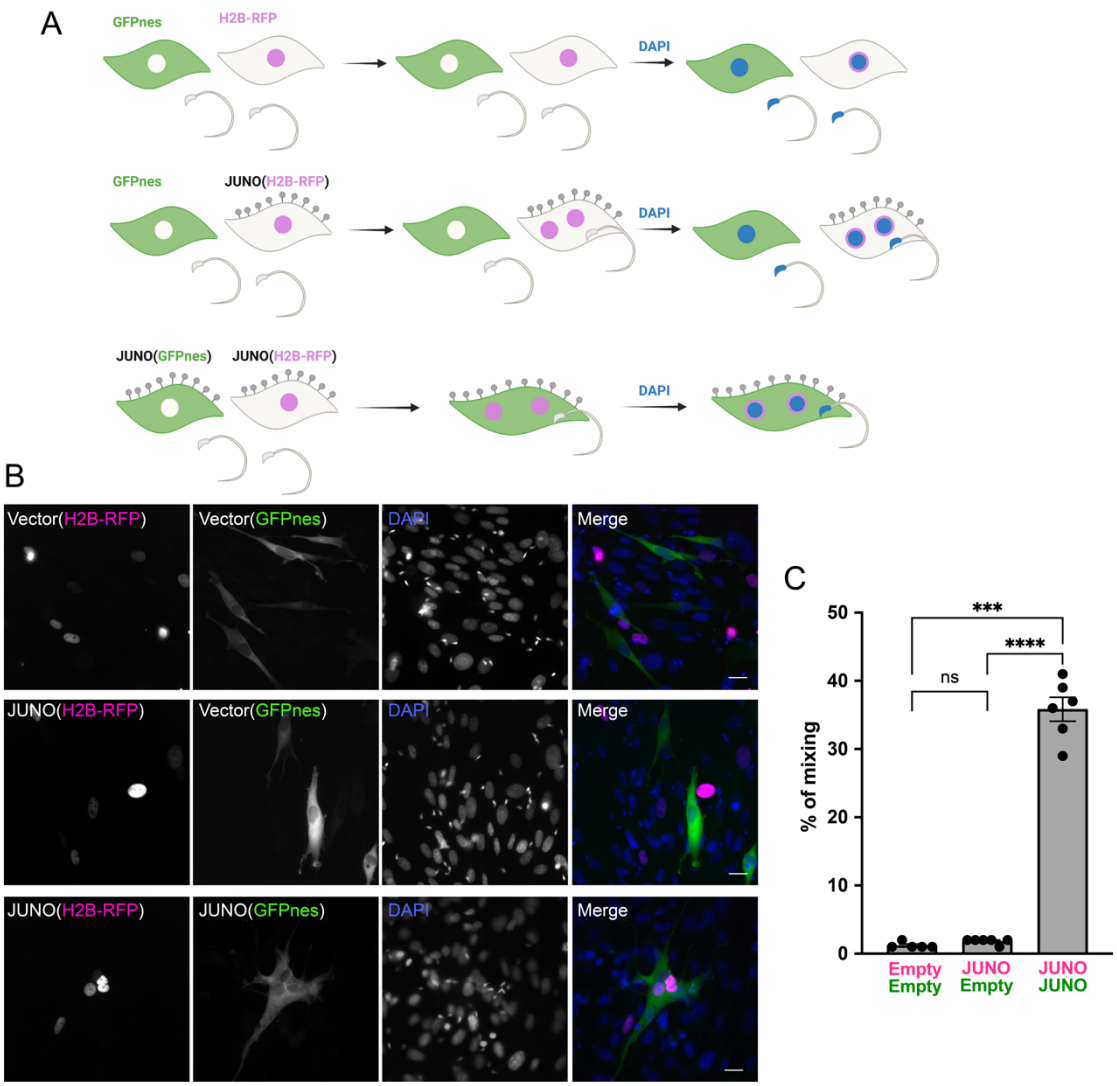

Figure 2: Sperm-induced fusion is dependent on JUNO

(A) Scheme of experimental design. BHK cells transfected with pCI::GFPnes or pCI::H2B-RFP empty vectors or containing the coding sequence for the expression of JUNO were mixed as indicated. Later, the cells were co-incubated with sperm for 4 h, fixed and stained with DAPI. (B) Representative images for each treatment. Each separate channel for GFPnes (green cytoplasm), H2B-RFP (magenta nuclei) and DAPI staining (blue) are shown. Scale bars, 20 µm. Fused, mixed cells contain both GFPnes and H2B-RFP staining. (C) Quantification of content mixing experiments. The percentage of mixing was defined as the ratio between the nuclei in mixed cells (NuM) and the total number of nuclei in mixed cells and fluorescent cells in contact that did not fuse (NuC), as follows: % of mixing = (NuM/[NuM + NuC]) × 100. Bar chart showing individual experiment values (each corresponding to 1,000 nuclei) and means ± SEM of six independent experiments. Comparisons by one-way ANOVA followed by Tukey's test. ns = non-significant, ***P < 0.001, ****P < 0.0001.

494

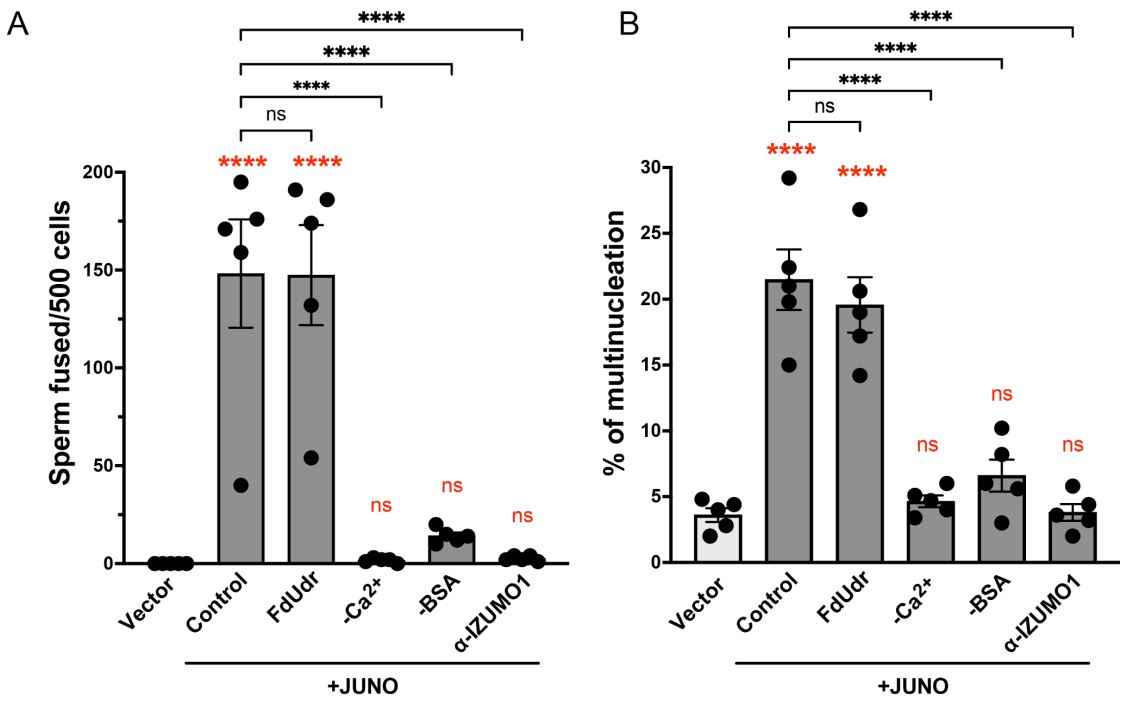

495

496 Figure 3: Syncytia formation requires a functional sperm, is dependent on IZUMO1
497 and is not affected by an inhibitor of cell division

498 BHK cells were transfected with pcDNA3.1-EGFP-MBD-nls together with pCI::H2B-
499 RFP (empty vector) or pCI::JUNO::H2B-RFP and co-incubated with control sperm in
500 the presence of 20 µM of the inhibitor of cell division FdUdr or of 1 µg/µl of anti-IZUMO1
501 antibody (clone Mab120). Alternatively, cells were mixed with sperm incubated in a
502 medium lacking calcium (-Ca^{2+}) or bovine serum albumin (-BSA); both conditions fail
503 to support sperm capacitation. The number of sperm fused per 500 fluorescent cells
504 **(A)** and the percentage of multinucleation **(B)** were determined. Bar charts showing
505 individual experiment values and means ± SEM of five independent experiments.
506 Comparisons by one-way ANOVA followed by Tukey's test. In red are the comparisons
507 against the empty vector. ns = non-significant, ***P < 0.001, ****P < 0.0001.

508

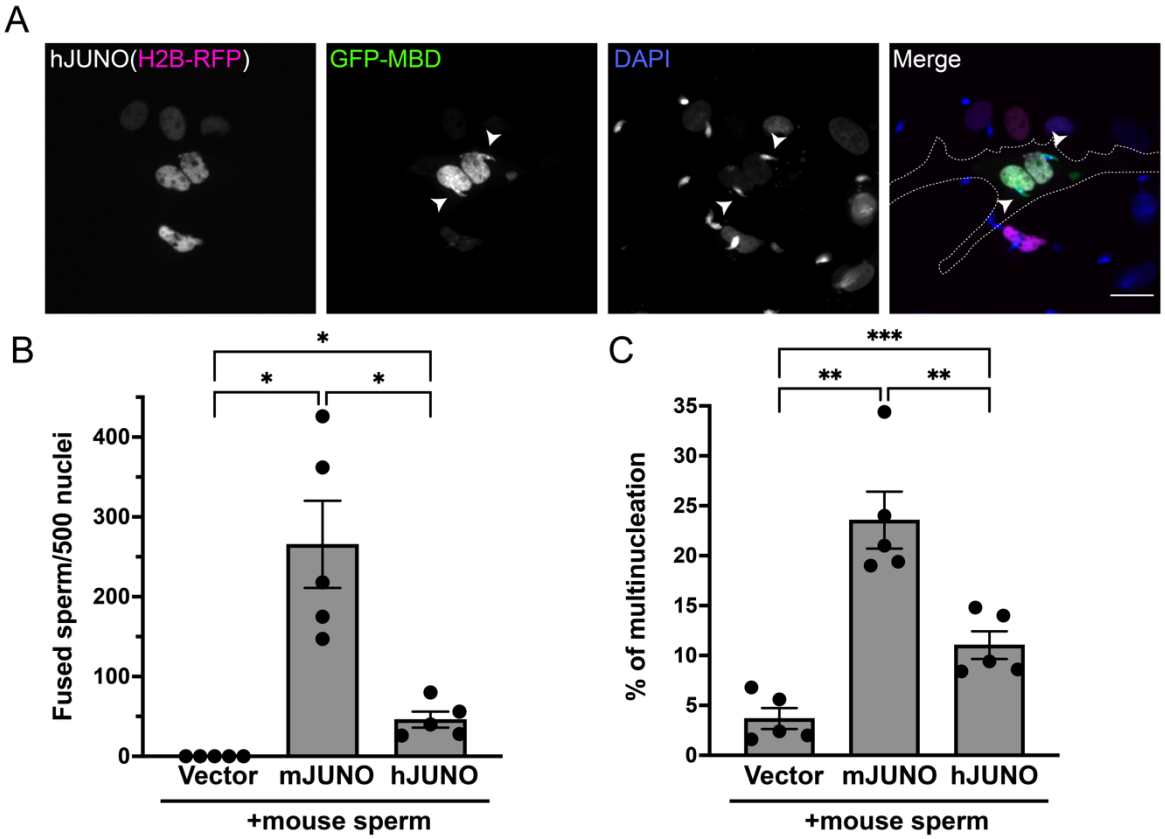

Figure 4: Sperm induce BHK-BHK fusion in a species-specific manner.

BHK cells were transfected with pcDNA3.1-EGFP-MBD-nls together pCI::H2B-RFP (empty vector) or pCI::JUNO::H2B-RFP encoding for human JUNO (hJUNO) or mouse JUNO (mJUNO), and co-incubated with capacitated mouse sperm. **(A)** Representative images showing H2B-RFP (magenta), GFP-MBD (green), DAPI (blue) channels and the merge. Dotted lines contour a cell transfected with human JUNO with two mouse sperm fused (arrowheads). Scale bar, 20 µm. The number of sperm fused per 500 fluorescent cells **(B)** and the percentage of multinucleation **(C)** were determined. Bar charts showing individual experiment values and means ± SEM of five independent experiments. Comparisons by one-way ANOVA followed by Tukey's test. *P < 0.05, **P < 0.01, ***P < 0.001.

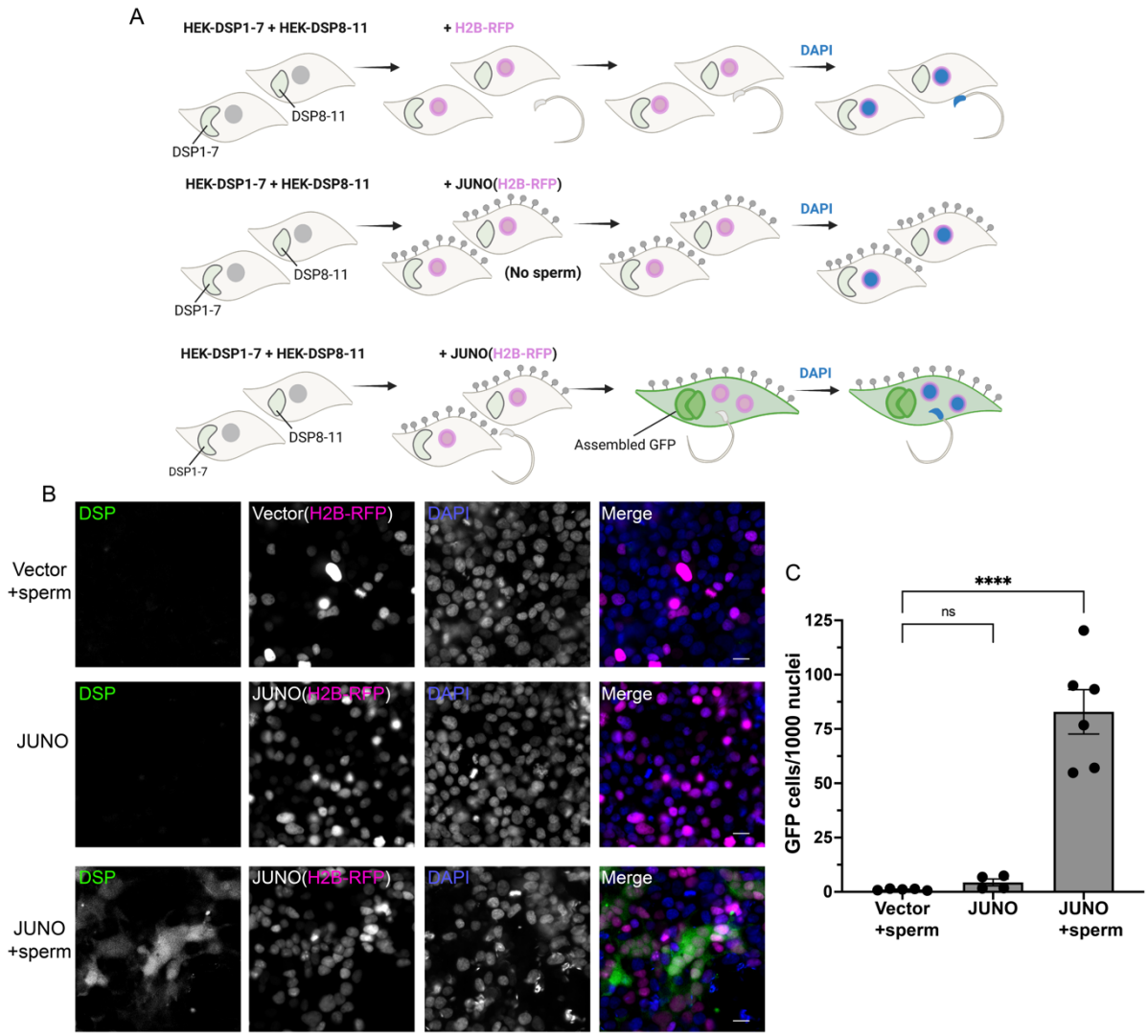

522

523 Figure 5: Sperm-induced fusion of human cells evaluated by Dual Split Proteins
524 (DSP)

525 (A) Scheme of experimental design. HEK293T cells stably expressing the split GFP
526 (DSP1-7 or DSP8-11) were mixed and transfected with pCI::H2B-RFP or
527 pCI::JUNO::H2B-RFP vectors. When indicated, the cells were later co-incubated with
528 sperm for 4 h, fixed and stained with DAPI. (B) Representative images for each
529 treatment. Each separate channel for GFP (assembled GFP in fused cells), H2B-RFP
530 (magenta nuclei) and DAPI staining (blue) are shown. Scale bars, 20 µm. (C)
531 Quantification of content mixing experiments. The extent of fusion was determined by
532 counting the number of GFP positive cells per 1,000 nuclei. Bar chart showing
533 individual experiment values (each corresponding to 1,000 to 2,000 nuclei) and means
534 ± SEM of at least four independent experiments. Comparisons by one-way ANOVA
535 followed by Tukey's test. ns = non-significant, ****P < 0.0001.

536

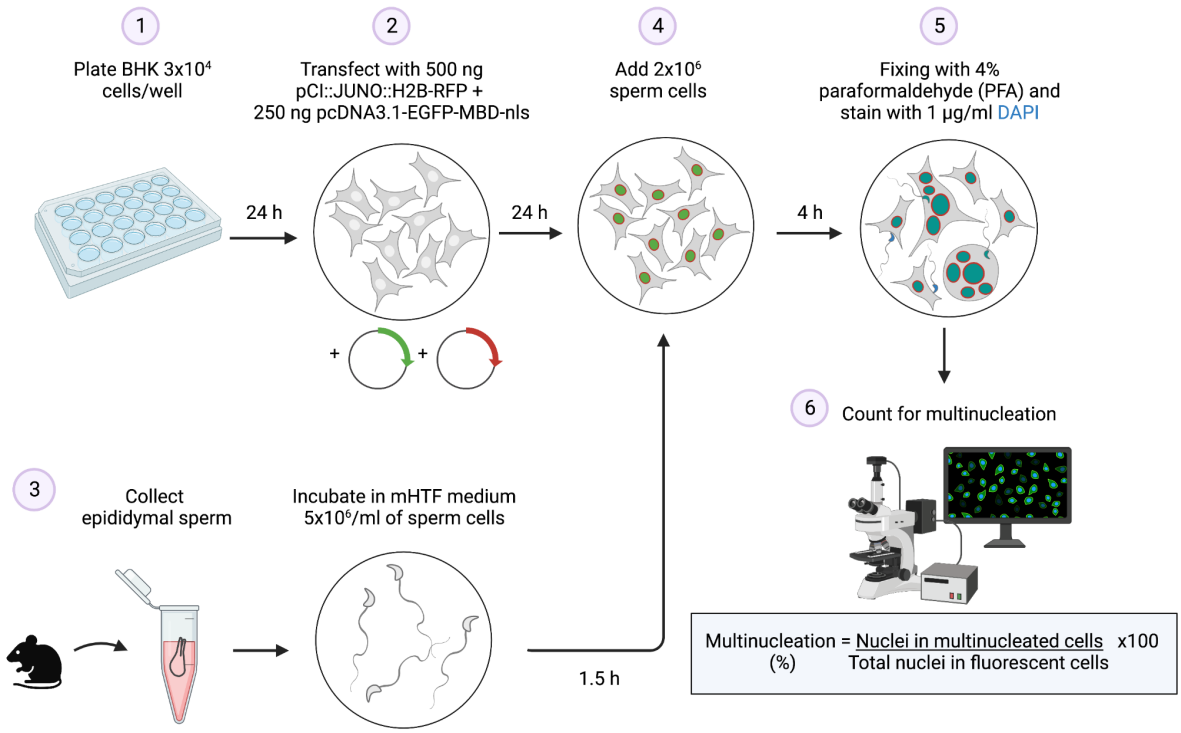

Figure 6: Summary of the SPICER method

Schematic representation of the multinucleation assay employed to determine the sperm fusogenic potential. (1) BHK are seeded on a plate. (2) The cells are transfected with the plasmids encoding for JUNO and EGFP-MBD. (3) Mouse sperm cells are collected and capacitated. (4) The BHK and sperm cells are co-incubated. (5) The cells are washed, fixed and stained with DAPI. (6) Multinucleation levels are quantified as indicated.

546 **Supplementary Information**

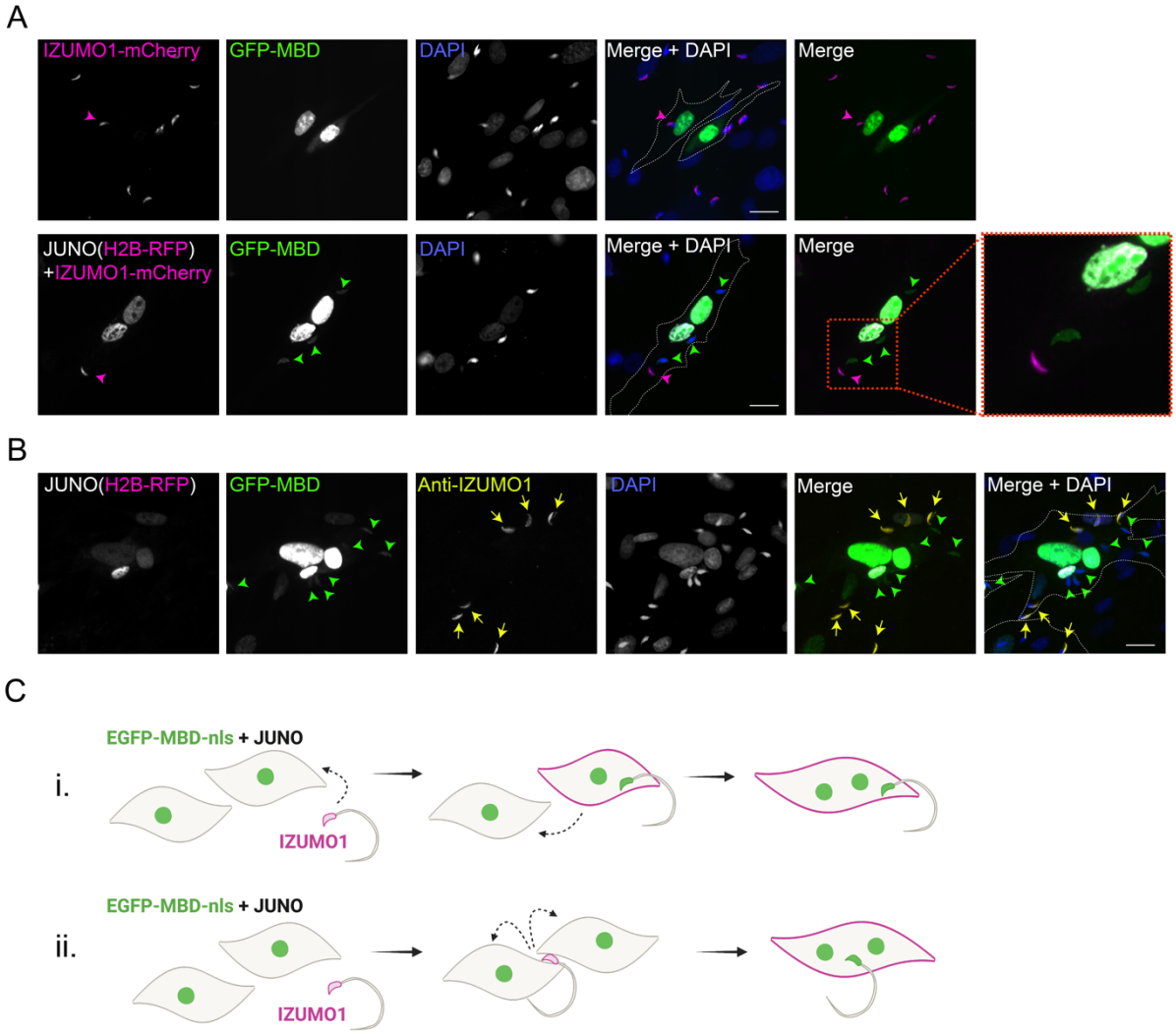

547

548 Figure S1: IZUMO1 diffuses into the target cell upon sperm fusion

549 **(A)** BHK were transfected with pcDNA3.1-EGFP-MBD-nls alone or together with
550 pCI::JUNO::H2B-RFP and co-incubated with sperm obtained from transgenic mice
551 expressing IZUMO1-mcherry. Representative images showing H2B-RFP and Izumo1-
552 mCherry (magenta), GFP-MBD (green), DAPI (blue) channels and the merge with and
553 without DAPI. Dotted lines contour relevant cells. Scale bar, 20 µm. Magenta
554 arrowheads point to unfused sperm (GFP negative) presenting IZUMO1-mCherry
555 signal while green arrowheads point to fused sperm (GFP positive) without Izumo1-
556 mCherry signal. **(B)** BHK were transfected with pcDNA3.1-EGFP-MBD-nls together
557 with pCI::JUNO::H2B-RFP and co-incubated with wild-type mouse sperm. After
558 fixation, an immunostaining against IZUMO1 was performed. Representative images
559 showing H2B-RFP (magenta), GFP-MBD (green), IZUMO1 staining (yellow), DAPI
560 (blue) channels and the merge with and without DAPI. Dotted lines contour relevant
561 cells. Scale bar, 20 µm. Yellow arrows point to unfused sperm (GFP negative)

562 presenting IZUMO1 signal while green arrowheads point to fused sperm (GFP
563 positive) without IZUMO1 signal. **(C)** Models for sperm-induced cell-cell fusion. In
564 general, this phenomenon resembles the so-called “fusion from without” in which
565 viruses can induce the fusion of the target cells (Falke, Knoblich, and Müller 1985;
566 Tang et al. 2021; Edwards and Brown 1986). i- One sperm fuses with a BHK, IZUMO1
567 is transferred by diffusion and mediates the fusion to another cell. ii- One sperm fuses
568 to two BHK bridging them and inducing the formation of a syncytium.

569

570

571 **Movie S1:** Time-lapse experiment using spinning disk confocal microscopy showing
572 the fusion of two cells expressing JUNO and GFPnes after the addition of sperm at
573 t=0 min. Time in hours:minutes. Green and DIC channels are shown. Scale bars, 20
574 µm.

575

References

Abay, Zehra C., Michelle Yu-Ying Wong, Jean-Sébastien Teoh, Tarika Vijayaraghavan, Massimo A. Hilliard, and Brent Neumann. 2017. "Phosphatidylserine Save-Me Signals Drive Functional Recovery of Severed Axons in Caenorhabditis Elegans." *Proceedings of the National Academy of Sciences of the United States of America* 114 (47): E10196–205.

Aitken, R. J., and R. A. Elton. 1986. "Quantitative Analysis of Sperm-Egg Interaction in the Zona-Free Hamster Egg Penetration Test." *International Journal of Andrology* 9 (s6): 14–30.

Allingham, Jessica, and Wely B. Floriano. 2021. "Genetic Diversity in the IZUMO1-JUNO Protein-Receptor Pair Involved in Human Reproduction." *PloS One* 16 (12): e0260692.

Aydin, Halil, Azmiri Sultana, Sheng Li, Annoj Thavalingam, and Jeffrey E. Lee. 2016. "Molecular Architecture of the Human Sperm IZUMO1 and Egg JUNO Fertilization Complex." *Nature* 534 (7608): 562–65.

Barbaux, Sandrine, Côme Ialy-Radio, Myriam Chalbi, Elisa Dybal, Méline Homps-Legrand, Marcio Do Cruzeiro, Daniel Vaiman, Jean-Philippe Wolf, and Ahmed Ziyyat. 2020. "Sperm SPACA6 Protein Is Required for Mammalian Sperm-Egg Adhesion/Fusion." *Scientific Reports* 10 (1): 5335.

Bendich, A., E. Borenfreund, and S. S. Sternberg. 1974. "Penetration of Somatic Mammalian Cells by Sperm." *Science* 183 (4127): 857–59.

Bianchi, Enrica, Brendan Doe, David Goulding, and Gavin J. Wright. 2014. "Juno Is the Egg Izumo Receptor and Is Essential for Mammalian Fertilization." *Nature* 508: 483–87.

Bianchi, Enrica, and Gavin J. Wright. 2015. "Cross-Species Fertilization: The Hamster Egg Receptor, Juno, Binds the Human Sperm Ligand, Izumo1." *Philosophical Transactions of the Royal Society of London. Series B, Biological Sciences* 370(1661): 20140101.

Binner, Mirjam I., Anna Kogan, Karin Panser, Alexander Schleiffer, Victoria E. Deneke, and Andrea Pauli. 2021. "The Sperm Protein Spaca6 Is Essential for Fertilization in Zebrafish." *Frontiers in Cell and Developmental Biology* 9: 806982.

Bratt, Michael A., and William R. Gallaher. 1969. "Preliminary analysis of the requirements for fusion from within and fusion from without by newcastle disease virus*." *Proceedings of the National Academy of Sciences* 64 (2): 536–43.

Brukman, Nicolas G., Xiaohui Li, and Benjamin Podbilewicz. 2022. "Fusexins, HAP2/GCS1 and Evolution of Gamete Fusion." *Frontiers in Cell and Developmental Biology* 9: 824024.

Brukman, Nicolas G., Kohdai P. Nakajima, Clari Valansi, Kateryna Flyak, Xiaohui Li, Tetsuya Higashiyama, and Benjamin Podbilewicz. 2023. "A Novel Function for the Sperm Adhesion Protein IZUMO1 in Cell-Cell Fusion." *J Cell Biol. 2023 Feb 6;222(2):e202207147.*

Brukman, Nicolas G., Berna Uygur, Benjamin Podbilewicz, and Leonid V. Chernomordik. 2019. "How Cells Fuse." *J Cell Biol.* 218 (5): 1436–51.

Buchrieser, Julian, Jérémy Dufloo, Mathieu Hubert, Blandine Monel, Delphine Planas, Maaran Michael Rajah, Cyril Planchais, et al. 2020. "Syncytia Formation by SARS-CoV-2-Infected Cells." *The EMBO Journal* 39 (23): e106267.

Ciechonska, Marta, Tim Key, and Roy Duncan. 2014. "Efficient Reovirus- and Measles Virus-Mediated Pore Expansion during Syncytium Formation Is Dependent on Annexin A1 and Intracellular Calcium." *Journal of Virology* 88 (11): 6137–47.

Clark, Sydney, and Rajesh K. Naz. 2013. “Presence and Incidence of Izumo Antibodies in Sera of Immunoinfertile Women and Men.” *Am J Reprod Immunol. 2013 Mar;69(3):256-63.*

Deneke, Victoria E., and Andrea Pauli. 2021. “The Fertilization Enigma: How Sperm and Egg Fuse.” *Annual Review of Cell and Developmental Biology* 37 (October): 391–414.

Duelli, Dominik, and Yuri Lazebnik. 2007. “Cell-to-Cell Fusion as a Link between Viruses and Cancer.” *Nature Reviews. Cancer* 7 (12): 968–76.

Earles, C. A., J. Bai, P. Wang, and E. R. Chapman. 2001. “The Tandem C2 Domains of Synaptotagmin Contain Redundant Ca2+ Binding Sites That Cooperate to Engage T-SNAREs and Trigger Exocytosis.” *The Journal of Cell Biology* 154 (6): 1117–23.

Edwards, J., and D. T. Brown. 1986. “Sindbis Virus-Mediated Cell Fusion from without Is a Two-Step Event.” *The Journal of General Virology* 67 (Pt 2) (February): 377–80.

Eigler, Tamar, Giulia Zarfati, Emmanuel Amzallag, Sansrity Sinha, Nadav Segev, Yishaia Zabary, Assaf Zaritsky, et al. 2021. “ERK1/2 Inhibition Promotes Robust Myotube Growth via CaMKII Activation Resulting in Myoblast-to-Myotube Fusion.” *Developmental Cell* 56 (24): 3349–63.e6.

Eijnde, S. M. van den, M. J. van den Hoff, C. P. Reutelingsperger, W. L. van Heerde, M. E. Henfling, C. Vermeij-Keers, B. Schutte, M. Borgers, and F. C. Ramaekers. 2001. “Transient Expression of Phosphatidylserine at Cell-Cell Contact Areas Is Required for Myotube Formation.” *Journal of Cell Science* 114 (Pt 20): 3631–42.

Enoiu, Simona Ioana, Marie Berg Nygaard, Mona Bungum, Søren Ziebe, Morten R. Petersen, and Kristian Almstrup. 2022. “Expression of Membrane Fusion Proteins in Spermatozoa and Total Fertilisation Failure during in Vitro Fertilisation.” *Andrology.* 2022 Oct;10(7):1317-1327.

Falke, D., A. Knoblich, and S. Müller. 1985. “Fusion from without Induced by Herpes Simplex Virus Type 1.” *Intervirology* 24 (4): 211–19.

Ferris, P. J., J. P. Woessner, and U. W. Goodenough. 1996. “A Sex Recognition Glycoprotein Is Encoded by the plus Mating-Type Gene fus1 of Chlamydomonas Reinhardtii.” *Molecular Biology of the Cell* 7 (8): 1235.

Fujihara, Yoshitaka, Yonggang Lu, Taichi Noda, Asami Oji, Tamara Larasati, Kanako Kojima-Kita, Zhifeng Yu, Ryan M. Matzuk, Martin M. Matzuk, and Masahito Ikawa. 2020. “Spermatozoa Lacking Fertilization Influencing Membrane Protein (FIMP) Fail to Fuse with Oocytes in Mice.” *Proceedings of the National Academy of Sciences of the United States of America* 117 (17): 9393–9400.

Gert, Krista R. B., Karin Panser, Joachim Surm, Benjamin S. Steinmetz, Alexander Schleiffer, Luca Jovine, Yehu Moran, Fyodor Kondrashov, and Andrea Pauli. 2023. “Divergent Molecular Signatures in Fish Bouncer Proteins Define Cross-Fertilization Boundaries.” *Nature Communications* 14 (1): 3506.

Grayson, Phil. 2015. “Izumo1 and Juno: The Evolutionary Origins and Coevolution of Essential Sperm–egg Binding Partners.” *R Soc Open Sci.* 2015 Dec 16;2(12):150296.

Herberg, Sarah, Krista R. Gert, Alexander Schleiffer, and Andrea Pauli. 2018. “The Ly6/uPAR Protein Bouncer Is Necessary and Sufficient for Species-Specific Fertilization.” *Science* 361 (6406): 1029.

Hino, Toshiaki, Yuko Muro, Miwa Tamura-Nakano, Masaru Okabe, Hiroyuki Tateno, and Ryuzo Yanagimachi. 2016. “The Behavior and Acrosomal Status of Mouse Spermatozoa In Vitro, and Within the Oviduct During Fertilization after Natural

675 Mating." *Biology of Reproduction* 95 (3): 50.
676 Inoue, Naokazu, Yoshihisa Hagihara, and Ikuo Wada. 2021. "Evolutionarily
677 Conserved Sperm Factors, DCST1 and DCST2, Are Required for Gamete
678 Fusion." *Elife.* 2021 Apr 19;10:e66313.
679 Inoue, Naokazu, Yoshihisa Hagihara, Danelle Wright, Takahisa Suzuki, and Ikuo
680 Wada. 2015. "Oocyte-Triggered Dimerization of Sperm IZUMO1 Promotes
681 Sperm-Egg Fusion in Mice." *Nature Communications* 6: 8858.
682 Inoue, Naokazu, Daizo Hamada, Hironari Kamikubo, Kunio Hirata, Mikio Kataoka,
683 Masaki Yamamoto, Masahito Ikawa, Masaru Okabe, and Yoshihisa Hagihara.
684 2013. "Molecular Dissection of IZUMO1, a Sperm Protein Essential for Sperm-
685 Egg Fusion." *Development* 140 (15): 3221–29.
686 Inoue, Naokazu, Masahito Ikawa, Ayako Isotani, and Masaru Okabe. 2005. "The
687 Immunoglobulin Superfamily Protein Izumo Is Required for Sperm to Fuse with
688 Eggs." *Nature* 434 (7030): 234–38.
689 Ishikawa, Hirohito, Fanxia Meng, Naoyuki Kondo, Aikichi Iwamoto, and Zene Matsuda.
690 2012. "Generation of a Dual-Functional Split-Reporter Protein for Monitoring
691 Membrane Fusion Using Self-Associating Split GFP." *Protein Engineering,*
692 *Design & Selection: PEDS* 25 (12): 813–20.
693 Kito, Seiji, Tatsuo Hayao, Yoshiko Noguchi-Kawasaki, Yuki Ohta, Uhara Hideki, and
694 Shintaro Tateno. 2004. "Improved in Vitro Fertilization and Development by Use
695 of Modified Human Tubal Fluid and Applicability of Pronucleate Embryos for
696 Cryopreservation by Rapid Freezing in Inbred Mice." *Comparative Medicine* 54
697 (5): 564–70.
698 Kohn, A. 1965. "Polykaryocytosis induced by newcastle disease virus in monolayers
699 of animal cells." *Virology* 26 (June): 228–45.
700 Lamas-Toranzo, Ismael, Julieta G. Hamze, Enrica Bianchi, Beatriz Fernández-
701 Fuertes, Serafín Pérez-Cerezales, Ricardo Laguna-Barraza, Raúl Fernández-
702 González, et al. 2020. "TMEM95 Is a Sperm Membrane Protein Essential for
703 Mammalian Fertilization." *Elife.* 2020 Jun 2;9:e53913.
704 La Spina, Florenza A., Lis C. Puga Molina, Ana Romarowski, Alejandra M. Vitale,
705 Tomas L. Falzone, Dario Krapf, Noritaka Hirohashi, and Mariano G. Buffone.
706 2016. "Mouse Sperm Begin to Undergo Acrosomal Exocytosis in the Upper
707 Isthmus of the Oviduct." *Developmental Biology* 411 (2): 172–82.
708 Lorenzetti, Diego, Christophe Poirier, Ming Zhao, Paul A. Overbeek, Wilbur Harrison,
709 and Colin E. Bishop. 2014. "A Transgenic Insertion on Mouse Chromosome 17
710 Inactivates a Novel Immunoglobulin Superfamily Gene Potentially Involved in
711 Sperm-Egg Fusion." *Mammalian Genome: Official Journal of the International*
712 *Mammalian Genome Society* 25: 141–48.
713 Lu, Yonggang, and Masahito Ikawa. 2022. "Eukaryotic Fertilization and Gamete
714 Fusion at a Glance." *Journal of Cell Science* 135 (22).
715 https://doi.org/10.1242/jcs.260296.
716 Matsumura, Takafumi, Taichi Noda, Yuhkoh Satouh, Akane Morohoshi, Shunsuke
717 Yuri, Masaki Ogawa, Yonggang Lu, Ayako Isotani, and Masahito Ikawa. 2021.
718 "Sperm IZUMO1 Is Required for Binding Preceding Fusion with Oolemma in Mice
719 and Rats." *Frontiers in Cell and Developmental Biology* 9: 3849.
720 Mattioli, M., A. Gloria, A. Mauro, L. Gioia, and B. Barboni. 2009. "Fusion as the Result
721 of Sperm-Somatic Cell Interaction." *Reproduction* 138 (4): 679–87.
722 Moi, David, Shunsuke Nishio, Xiaohui Li, Clari Valansi, Mauricio Langleib, Nicolas G.
723 Brukman, Kateryna Flyak, et al. 2022. "Discovery of Archaeal Fusexins
724 Homologous to Eukaryotic HAP2/GCS1 Gamete Fusion Proteins." *Nature*

Communications 13 (1): 3880.
Muro, Yuko, Hidetoshi Hasuwa, Ayako Isotani, Haruhiko Miyata, Kazuo Yamagata, Masahito Ikawa, Ryuzo Yanagimachi, and Masaru Okabe. 2016. “Behavior of Mouse Spermatozoa in the Female Reproductive Tract from Soon after Mating to the Beginning of Fertilization.” *Biology of Reproduction* 94 (4): 80.
Nakane, Shuhei, and Zene Matsuda. 2015. “Dual Split Protein (DSP) Assay to Monitor Cell-Cell Membrane Fusion.” In *Cell Fusion: Overviews and Methods: Second Edition*, Second, 229–36. Springer New York.
Nakajima KP, Valansi C, Kurihara D, Sasaki N, Podbilewicz B, Higashiyama T. Live imaging-based assay for visualising species-specific interactions in gamete adhesion molecules. Sci Rep. 2022 Jun 10;12(1):9609.
Nishimura, Hitoshi, Tatsuya Tajima, Heather Skye Comstra, Elizabeth J. Gleason, and Steven W. L’Hernault. 2015. “The Immunoglobulin-like Gene Spe-45 Acts during Fertilization in Caenorhabditis Elegans like the Mouse Izumo1 Gene.” *Current Biology: CB* 25 (24): 3225.
Nishimura, Kaoru, Ling Han, Enrica Bianchi, Gavin J. Wright, Daniele de Sanctis, and Luca Jovine. 2016. “The Structure of Sperm Izumo1 Reveals Unexpected Similarities with Plasmodium Invasion Proteins.” *Current Biology: CB* 26 (14): R661–62.
Noda, Taichi, Andreas Blaha, Yoshitaka Fujihara, Krista R. Gert, Chihiro Emori, Victoria E. Deneke, Seiya Oura, et al. 2022. “Sperm Membrane Proteins DCST1 and DCST2 Are Required for Sperm-Egg Interaction in Mice and Fish.” *Communications Biology* 5 (1): 332.
Noda, Taichi, Yonggang Lu, Yoshitaka Fujihara, Seiya Oura, Takayuki Koyano, Sumire Kobayashi, Martin M. Matzuk, and Masahito Ikawa. 2020. “Sperm Proteins SOF1, TMEM95, and SPACA6 Are Required for Sperm-Oocyte Fusion in Mice.” *Proceedings of the National Academy of Sciences of the United States of America* 117 (21): 11493–502.
Ohto, Umeharu, Hanako Ishida, Elena Krayukhina, Susumu Uchiyama, Naokazu Inoue, and Toshiyuki Shimizu. 2016. “Structure of IZUMO1–JUNO Reveals Sperm–oocyte Recognition during Mammalian Fertilization.” *Nature* 534 (7608): 566–69.
Okada, Y. 1962. “Analysis of Giant Polynuclear Cell Formation Caused by HVJ Virus from Ehrlich’s Ascites Tumor Cells. I. Microscopic Observation of Giant Polynuclear Cell Formation.” *Experimental Cell Research* 26 (February): 98–107.
Palermo, G., H. Joris, P. Devroey, and A. C. Van Steirteghem. 1992. “Pregnancies after Intracytoplasmic Injection of Single Spermatozoon into an Oocyte.” *The Lancet* 340 (8810): 17–18.
Pinello, Jennifer F., Yanjie Liu, and William J. Snell. 2021. “MAR1 Links Membrane Adhesion to Membrane Merger during Cell-Cell Fusion in Chlamydomonas.” *Dev Cell. 2021 Dec 20;56(24):3380-3392.e9.*
Practice Committees of the American Society for Reproductive Medicine and the Society for Assisted Reproductive Technology. 2020. “Intracytoplasmic Sperm Injection (ICSI) for Non-Male Factor Indications: A Committee Opinion.” *Fertility and Sterility* 114 (2): 239–45.
Rival, Claudia M., Wenhao Xu, Laura S. Shankman, Sho Morioka, Sanja Arandjelovic, Chang Sup Lee, Karen M. Wheeler, et al. 2019. “Phosphatidylserine on Viable Sperm and Phagocytic Machinery in Oocytes Regulate Mammalian Fertilization.” *Nature Communications* 10 (1): 4456.
Satouh, Yuhkoh, Naokazu Inoue, Masahito Ikawa, and Masaru Okabe. 2012.

775 "Visualization of the Moment of Mouse Sperm-Egg Fusion and Dynamic
776 Localization of IZUMO1." *Journal of Cell Science* 125 (Pt 21): 4985–90.
777 Shilagardi, Khurts, Shuo Li, Fengbao Luo, Faiz Marikar, Rui Duan, Peng Jin, Ji Hoon
778 Kim, Katherine Murnen, and Elizabeth H. Chen. 2013. "Actin-Propelled Invasive
779 Membrane Protrusions Promote Fusogenic Protein Engagement during Cell-Cell
780 Fusion." *Science* 340 (6130): 359–63.
781 Spiegelstein, O., J. D. Eudy, and R. H. Finnell. 2000. "Identification of Two Putative
782 Novel Folate Receptor Genes in Humans and Mouse." *Gene* 258 (1-2): 117–25.
783 Stepanenko, Nataliia, Omri Wolk, Enrica Bianchi, Gavin James Wright, Natali
784 Schachter-Safrai, Kiril Makedonski, Alberto Ouro, Assaf Ben-Meir, Yosef
785 Buganim, and Amiram Goldblum. 2022. "In Silico Docking Analysis for Blocking
786 JUNO-IZUMO1 Interaction Identifies Two Small Molecules That Block in Vitro
787 Fertilization." *Frontiers in Cell and Developmental Biology* 10 (April): 824629.
788 Steptoe, P. C., and R. G. Edwards. 1978. "Birth after the Reimplantation of a Human
789 Embryo." *The Lancet* 2 (8085): 366.
790 Suzuki, Banri, Yukou Sugano, Jun Ito, Haruka Saito, Sueo Niimura, and Hideaki
791 Yamashiro. 2017. "Location and Expression of Juno in Mice Oocytes during
792 Maturation." *JBRA Assisted Reproduction* 21 (4): 321–26.
793 Takaiso, Nobue, Haruki Nishizawa, Sachie Nishiyama, Tomio Sawada, Eriko Hosoba,
794 Tamae Ohye, Tsutomu Sato, Hidehito Inagaki, and Hiroki Kurahashi. 2016.
795 "Mutation Analysis of the *JUNO* Gene in Female Infertility of Unknown Etiology."
796 *Fujita Medical Journal* 2 (3): 59–61.
797 Takayama, Jun, Tatsuya Tajima, Shuichi Onami, and Hitoshi Nishimura. 2021. "C.
798 Elegans Spermatozoa Lacking Spe-45 Are Incapable of Fusing with the Oocyte
799 Plasma Membrane." *MicroPubl Biol.* 2021: 10.17912/micropub.biology.000372.
800 Tang, Jiajia, Giada Frascaroli, Xuan Zhou, Jan Knickmann, and Wolfram Brune. 2021.
801 "Cell Fusion and Syncytium Formation in Betaherpesvirus Infection." *Viruses.*
802 2021 Oct; 13(10): 1973.
803 Tateno, Hiroyuki, Dario Krapf, Toshiaki Hino, Claudia Sánchez-Cárdenas, Alberto
804 Darszon, Ryuzo Yanagimachi, and Pablo E. Visconti. 2013. "Ca2+ Ionophore
805 A23187 Can Make Mouse Spermatozoa Capable of Fertilizing in Vitro without
806 Activation of cAMP-Dependent Phosphorylation Pathways." *Proceedings of the*
807 *National Academy of Sciences of the United States of America* 110 (46): 18543–
808 48.
809 Theuerkauf, Samuel A., Alexander Michels, Vanessa Riechert, Thorsten J. Maier,
810 Egbert Flory, Klaus Cichutek, and Christian J. Buchholz. 2021. "Quantitative
811 Assays Reveal Cell Fusion at Minimal Levels of SARS-CoV-2 Spike Protein and
812 Fusion from without." *iScience* 24 (3): 102170.
813 Tsuchiya, Masaki, Yuji Hara, Masaki Okuda, Karin Itoh, Ryotaro Nishioka, Akifumi
814 Shiomi, Kohjiro Nagao, et al. 2018. "Cell Surface Flip-Flop of Phosphatidylserine
815 Is Critical for PIEZO1-Mediated Myotube Formation." *Nature Communications* 9
816 (1): 2049.
817 Valansi, Clari, David Moi, Evgenia Leikina, Elena Matveev, Martín Graña, Leonid V.
818 Chernomordik, Héctor Romero, Pablo S. Aguilar, and Benjamin Podbilewicz.
819 2017. "Arabidopsis HAP2/GCS1 Is a Gamete Fusion Protein Homologous to
820 Somatic and Viral Fusogens." *The Journal of Cell Biology* 216: 571–81.
821 Vance, Tyler D. R., and Jeffrey E. Lee. 2020. "Virus and Eukaryote Fusogen
822 Superfamilies." *Current Biology: CB* 30 (13): R750–54.
823 Verma, Santosh K., Evgenia Leikina, Kamran Melikov, Claudia Gebert, Vardit Kram,
824 Marian F. Young, Berna Uygur, and Leonid V. Chernomordik. 2018. "Cell-Surface

825 Phosphatidylserine Regulates Osteoclast Precursor Fusion." *The Journal of*
826 *Biological Chemistry* 293 (1): 254–70.
827 Visconti, Pablo E., Janice L. Bailey, Grace D. Moore, Dieyun Pan, Patricia Olds-
828 Clarke, and Gregory S. Kopf. 1995. "Capacitation of Mouse Spermatozoa. I.
829 Correlation between the Capacitation State and Protein Tyrosine
830 Phosphorylation." *Development* 121: 1129–37.
831 Wang, Hongyun, Xiao Li, Shuhei Nakane, Shujun Liu, Hirohito Ishikawa, Aikichi
832 Iwamoto, and Zene Matsuda. 2014. "Co-Expression of Foreign Proteins Tethered
833 to HIV-1 Envelope Glycoprotein on the Cell Surface by Introducing an Intervening
834 Second Membrane-Spanning Domain." *PloS One* 9 (5): e96790.
835 Wengler, G. 1975. "Studies on the Synthesis of Viral RNA-Polymerase-Template
836 Complexes in BHK 21 Cells Infected with Semliki Forest Virus." *Virology* 66 (1):
837 322–26.
838 Williams, Ruth M., Upeka Senanayake, Mara Artibani, Gunes Taylor, Daniel Wells,
839 Ahmed Ashour Ahmed, and Tatjana Sauka-Spengler. 2018. "Genome and
840 Epigenome Engineering CRISPR Toolkit for in Vivo Modulation of Cis-Regulatory
841 Interactions and Gene Expression in the Chicken Embryo." *Development* 145 (4).
842 https://doi.org/10.1242/dev.160333.
843 Wood, Laura, and Gavin J. Wright. 2019. "High-Content Imaging for Large-Scale
844 Detection of Low-Affinity Extracellular Protein Interactions." *SLAS Discovery :*
845 *Advancing Life Sciences R & D* 24 (10): 987–99.
846 World Health Organization. 2023. *Infertility Prevalence Estimates, 1990–2021*. Edited
847 by World Health Organization. Geneva.
848 World Health Organization, HRP. 2021. "WHO Laboratory Manual for the Examination
849 and Processing of Human Semen." Sixth Edition. World Health Organization.
850 Yamagata, Kazuo, Taiga Yamazaki, Misuzu Yamashita, Yuki Hara, Narumi Ogonuki,
851 and Atsuo Ogura. 2005. "Noninvasive Visualization of Molecular Events in the
852 Mammalian Zygote." *Genesis* 43 (2): 71–79.
853 Yamaguchi, Tomoyuki, Keiji Hirota, Kanji Nagahama, Katsuya Ohkawa, Takeshi
854 Takahashi, Takeshi Nomura, and Shimon Sakaguchi. 2007. "Control of Immune
855 Responses by Antigen-Specific Regulatory T Cells Expressing the Folate
856 Receptor." *Immunity* 27 (1): 145–59.
857 Yanagimachi, R., H. Yanagimachi, and B. J. Rogers. 1976. "The Use of Zona-Free
858 Animal Ova as a Test-System for the Assessment of the Fertilizing Capacity of
859 Human Spermatozoa." *Biology of Reproduction* 15 (4): 471–76.
860 Yanagimachi, Ryuzo. 1988. "Chapter 1 Sperm–Egg Fusion." In *Current Topics in*
861 *Membranes and Transport*, edited by Felix Bronner, 32:3–43. Academic Press.
862 Yanagimachi, Ryuzo. 2022. "Mysteries and Unsolved Problems of Mammalian
863 Fertilization and Related Topics." *Biology of Reproduction* 106 (4): 644–75.
864 Yang, Yihong, Yan Zhang, Wen Jun Li, Yuxiang Jiang, Zhiwen Zhu, Huifang Hu, Wei
865 Li, et al. 2017. "Spectraplakin Induces Positive Feedback between Fusogens and
866 the Actin Cytoskeleton to Promote Cell-Cell Fusion." *Developmental Cell* 41 (1):
867 107–20.e4.
868 Yu, Mengru, Han Zhao, Tailai Chen, Ye Tian, Mei Li, Keliang Wu, Yuehong Bian, et
869 al. 2018. "Mutational Analysis of IZUMO1R in Women with Fertilization Failure
870 and Polyspermy after in Vitro Fertilization." *Journal of Assisted Reproduction and*
871 *Genetics* 35 (3): 539–44.
872 Zainul Rashid, M. R., S. B. Fishel, S. Thornton, J. A. Hall, G. Ndukwe, M. Aloum, and
873 S. D. Fleming. 1998. "The Predictive Value of the Zona-Free Hamster Egg
874 Penetration Test in Relation to in-Vitro Fertilization at Various Insemination

875 Concentrations." *Human Reproduction* 13 (3): 624–29.
876 Zhang, Yan, Yihong Yang, Zhiwen Zhu, and Guangshuo Ou. 2017. "WASP-Arp2/3-
877 Dependent Actin Polymerization Influences Fusogen Localization during Cell-Cell
878 Fusion in Caenorhabditis elegans Embryos." *Biology Open* 6 (9): 1324–28.